DOI: 10.7860/IJARS/2016/20857:2187

Original Article

Radiology Section

# Role of DWI in Detection and Characterization of Focal Liver Lesions

MADHU SD, JAIPAL R BEERAPPA, POOJA, RAGHURAM P


## ABSTRACT

**Introduction:** With widespread use of imaging modalities including USG, triple Phase CT-scan and MRI, there is increase in rate of detecting focal liver lesions in otherwise asymptomatic patient. This poses a diagnostic challenge in an Oncology patient as their accurate diagnosis is must for proper staging in a patient with known oncological disease. The accurate diagnosis of these focal liver lesions requires either FNAC or biopsies. Even though all these modalities help in characterizing liver lesions, MRI is most accurate modality in characterizing these lesions, especially DWI sequence, which provides information at the molecular level of the tissue giving structural and functional information and also helps in assessing the treatment response in tumor cells.

**Aim:** To study the role of DWI/ADC in detecting focal liver lesions and its further characterization. Also, assessing its role in differentiating benign from malignant lesions using DWI/ADC map and providing a quantitative cut off ADC to differentiate benign from malignant lesions.

**Materials and Methods:** Total 50 patients with 71 liver lesions were evaluated with diffusion-weighted MR imaging for over a period of 2 years. All these lesions were assessed by experienced radiologist in the field of Onco-imaging. Necessary clinical history and laboratory data were considered and all lesions either biopsied or underwent FNAC for final Diagnosis. All cases underwent DWI at two different b values of b 600 and b 1000 and corresponding ADC were calculated for each lesion.

**Results:** For the current study total of 50 patients (71 liver lesions) were investigated, majority of patients were in age group of 41-60 years (48%). Out of 71 liver lesions, 40(56.3%) were malignant lesions and 31(43.7%) were benign lesions, with most common diagnosis being metastases 17 (34%) followed by HCC 12(24%) and simple cyst 10(20%).

**Conclusion:** Based on qualitative and quantitative assessment of liver lesions on DWI and ADC map, we could characterize liver lesions and differentiate malignant and benign lesions. DWI is a useful diagnostic tool in patients where contrast is contraindicated like in patients with renal impairment.


**Keywords:** ADC map, Biopsy, MRI, Triple phase CT.

## INTRODUCTION

Focal liver lesions pose a diagnostic challenge in an Oncology patient as their accurate diagnosis is must for proper staging in a patient with known oncological disease. With wide spread use of imaging modalities including USG, triple Phase CT scan and MRI, detecting focal liver lesions in otherwise asymptomatic patient is increasing, however their accurate diagnosis requires either FNAC or biopsies [1-4]. The frequency of detection these lesions varies from modality to modality, with CT scan detection rate is 7.2% - 33%, with MRI it is 10.2% - 34.5%, and with USG, it is 2.3% - 6.2% [5]. Even though all these modalities have high sensitivity of detecting these lesions, their specificity in characterizing these lesions varies with triple CECT and MR carrying highest specificity. Characterizing these lesions into benign and malignant on imaging remains diagnostic challenge. MRI is most accurate modality for characterizing these lesions because of its high soft tissue and contrast resolution and due to its newer functional modalities. DWI provides information at the molecular level of the tissue and it complements the morphological information provided by the conventional MRI and thus help in assessing the structures and function of the tissue and also in assessing the treatment response in tumor cells [6-9].

### Diffusion-Weighted MR Imaging – Principles

Diffusion Weighted Imaging (DWI) is one of the newer non-contrast imaging modality in MRI. It allows accurate lesion detection and characterization in liver due to its high

contrast resolution [4]. The principle of DWI is based on the assessment of random motion of water molecule in a tissue. Water molecular movement is thermally driven and completely random in totally unrestricted environment, this phenomenon is known as Brownian motion or free diffusion [10]. But molecular movement is not completely random in the biological tissues as their free movement is restricted due to their interaction with tissue compartment, cell membranes and intracellular organelles. These molecular movements within the tissue are categorized into intravascular, intracellular, or extracellular movements. The impedance to molecular movement is determined by the tissue cellularity, viscocity and presence of intact cell membranes. Restriction or impedance to molecular movement seen in tissue with high cellularity like tumor, in conditions with cytotoxic edema, abscess, and fibrosis. Increased molecular movement seen in tissue with low cellularity, vasogenic edema and in cells with disrupted cell membranes [9]. Thus DWI provides quantitative information about tissue microenvironment including its cellularity, tissue viscosity and cell membrane status.

DWI uses a basic T2 weighted spin echo sequence, which has a 90° RF pulse followed by 180° RF pulse, on either side of 180° refocusing pulse, two strong motion probing gradients are applied [Table/Fig-1]. Strength of the diffusion sensitizing gradient is termed as b value and is measured in seconds per square millimeter. By changing b value sensitivity of the diffusion sequence can be changed. ADC is calculated by performing DWI in two or more b values and MR systems automatically generates the ADC values, which are expressed in $mm^2$/sec. The calculated ADC values for all voxels are usually displayed over a parametric map. These ADC value measurements in the liver lesions can be used for lesion detection and characterization [11-16].

### Qualitative Assessment of DWI

DWI is performed in at least two b values, one at b value of 0 $sec/mm^2$ and other at higher b values of 500-1000 $sec/mm^2$ depending on body region being imaged. High signal intensity at high b value suggests restricted diffusion consistent with highly cellular tissue and low signal intensity at high b value suggests felicitated diffusion which indicates low cellular tissue or ruptured cell membranes. This signal change at different b values can be used for lesion detection and characterization [17].

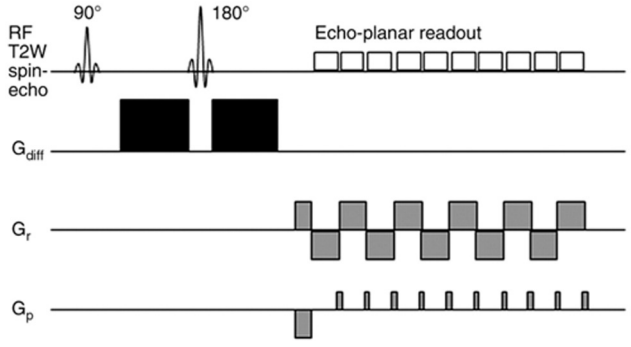


**[Table/Fig-1]:** EPI DWI sequences according to a Stejskal-Tanner experiment [11].

## MATERIALS AND METHODS

This study was conducted at Department of Radio-Diagnosis, Kidwai Memorial Institute of Oncology, from November 2012 to November 2013 after obtaining ethical committee clearance. Informed consent was obtained from all the patients, who were included in this study.

### Sample Size and Method

50 patients with 71 liver lesions were evaluated with diffusion-weighted MR imaging for a period of 2 years. Clinical history, biopsy/FNAC, laboratory findings (AFP level etc.,) and other imaging modalities like USG, CT Scan; wherever applicable were taken into consideration for final diagnosis of liver lesions.

### Inclusion Criteria

- Patients referred for MRI with clinically suspected liver lesions.
- Patients with liver lesions detected on USG or CT.

### Exclusion Criteria

- Patients having cardiac pacemakers, MRI incompatible prosthetic heart valves, cochlear implants or any metallic implants.
- Claustrophobic patients.
- Patients who cannot lay down- dyspnoeic patients and patients with severe backache.
- Pediatric/un-co-operative patients.

### Imaging Technique

All patients with focal liver lesions underwent either USG or CT scan for their detectin and were further referred to MRI for lesion characterization.

1. MR Imaging:

All patients were imaged in 1.5 Tesla Philips Achieva MRI machine in Torso XL coil. MRI done with atleast 4 hrs of fasting as contrast was used for triple phase study. Patients were given instructions about the examination and its time, and how to take and keep a deep breath. In supine position with arms extended above the head, Torso XL coil surface coil was placed over the upper abdomen. Respiratory-gated acquisitions were used wherever necessary.

2. Scan parameters [Table/Fig-2]:

| | |
|---|---|
| FOV | 220-300 mm |
| Matrix | 108 x 80 |
| Scan time | 3 minutes |
| Section thickness | 7 mm |
| Intersection gap | 1mm |
| Flip angle | 90 deg |
| NEX | 2 |
| TR | 1470 ms |
| TE | 68 ms |

**[Table/Fig-2]:** Scan parameters.

### Recommended Sequences

Fat suppressed single shot respiratory triggered EPI DWI sequence was performed in axial plane with 3D diffusion gradients by using three different b values (b=0 s/mm$^2$, b=500 s/mm$^2$ and b=1000 s/mm$^2$). Region of interest was drawn on ADC map to calculate ADC value. Axial T1 weighted and T2 weighted images were also obtained.

## STATISTICAL ANALYSIS

For statistical calculations, MedCalc v12.7.5.0 was used. Independent sample t-test and independent sample Welch-test for unequal variances were used. ROC curve analysis was done using MedCalc v12.7.5.0. The p-value of 0.05 or less was considered statistically significant.

## RESULTS

Total 50 cases were included in our study, among them 70% (35) were male patients and 30%(15) were female patients, majority of patients were in the age group of 41-60 years, followed by patients in the age group of 61-70 years with mean age of 52.3 years [Table/Fig-3]. In the current study, most of the patients had metastases (28 lesions) followed by HCC 12(24%) and simple cyst in 10(20%) patients and rest of the cases include hemangioma, hydatid cyst, abscess and adenoma. Of the total lesions, 56.3% were malignant and 43.7% were benign across population of 71% lesions and 70.4% lesions were observed in right hepatic lobe with 29.6% lesions in left hepatic lobe. Most of the lesions were predominantly observed in male patients, with 91.7% of HCCs and 80% of hemangiomas were seen in male population, simple cysts and hydatid cyst were equally seen both in males and females.

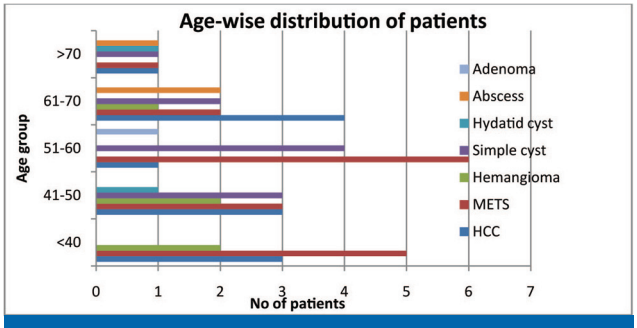


**[Table/Fig-3]:** Age wise distribution of cases.

In the current study 47 (88%) lesions were less than 5.0 cm in size, average size of lesion was 4.77cm. All 12 HCCs were greater than 5 cm in size and metastases were less than 5 cm size. In the present study, all HCCs (12 lesions) showed hyperintense signal on DWI at all 'b' values and hypointense signal on ADC map suggesting restricted diffusion. All metastases (28 lesions) showed similar findings as HCC, with hyperintense signal on DWI at all 'b' values and hypointense signal on ADC map. Thus, all HCCs and metastatic lesions in the study showed restricted diffusion. Heterogeneous hyperintense (DWI)/heterogeneous hypointense (ADC map) signal intensity was seen predominantly in necrotic lesions.

In the present study, out of total 9 hemangiomas, 8(89%) lesions showed hyperintense signal on DWI at all 'b' values. However, these lesions also showed hyperintense signal on ADC map suggesting no restricted diffusion. Persistence of hyperintense signal on higher 'b' values could be due to T2 shine through effect (validated by signal intensity on ADC map) [16,17]. One hemangioma lesion disappeared (showed hypointense signal) at b=1000sec/mm$^2$. Out of total 13 simple cysts, 4(30.8%) disappeared at b=500 sec/mm$^2$ and all lesions disappeared at b=1000sec/mm$^2$ on DWI. All lesions showed hyperintense signal intensity on ADC map (no restricted diffusion/showed facilitated diffusion). All the hydatid cysts (2 lesions) disappeared at b=1000 sec/mm$^2$ and showed hyperintense signal intensity on ADC map (no restricted diffusion). All abscesses (6 lesions) showed heterogeneous hyperintense signal intensity at b=500 sec/mm$^2$ and b=1000 sec/mm$^2$ and showed heterogeneous hypointense signal intensity on ADC map (restricted diffusion). This is due to high viscosity within the abscess core. Adenoma showed isointense signal intensity compared to surrounding liver parenchyma on DWI as well as ADC map.

In the current study with total 71 lesions, it was observed that benign lesions had highest mean ADC value. Hydatid cyst had max mean ADC value of $2.981\times10^{-3}$ mm$^2$/sec followed by simple cyst having $2.342\times10^{-3}$ mm$^2$/sec. Among malignant lesions HCC had the lowest mean ADC value of $0.975\times10^{-3}$ mm$^2$/sec while metastases had mean ADC value of $1.137\times10^{-3}$ mm$^2$/sec. [Table/Fig-4] shows the mean ADC values of all the lesions. Using Independent sample Welch-test for unequal variances; p-value < 0.05 therefore there was significant difference between mean ADC values for HCC and metastases. ADC cut-off value of 1.431x10$^{-3}$ mm$^2$/s was obtained by normal distribution (mean±2SD). ROC curve analysis (MedCalc v12.7.5.0 per Delong et al., [18] method)

| Type | Number of lesions | ADC in $10^{-3}$ mm²/s | | p value |
|---|---|---|---|---|
| | | Mean | SD | |
| Malignant | 40 | 1.08 | 0.25 | <0.001 |
| Benign | 31 | 1.87 | 0.72 | |

**[Table/Fig-3]:** Mean ADC of benign and malignant lesions

| Diagnosis | No of lesions | Mean ADC (x $10^{-3}$ mm²/ sec) | SD | 95% Confidence Interval for Mean | | Min ADC | Max ADC |
|---|---|---|---|---|---|---|---|
| | | | | Lower bound | Upper bound | (x $10^{-3}$ mm²/s) | (x $10^{-3}$ mm²/s) |
| HCC | 12 | 0.975 | 0.193 | 0.853 | 1.098 | 0.690 | 1.236 |
| METS | 28 | 1.137 | 0.260 | 1.035 | 1.238 | 0.625 | 1.598 |
| Hemangioma | 9 | 1.689 | 0.298 | 1.459 | 1.918 | 1.346 | 2.172 |
| Simple cyst | 13 | 2.342 | 0.441 | 2.076 | 2.609 | 1.669 | 3.208 |
| Hydatid cyst | 2 | 2.981 | 0.429 | - | - | 2.677 | 3.284 |
| Abscess | 6 | 0.879 | 0.230 | 0.638 | 1.121 | 0.532 | 1.244 |
| Adenoma | 1 | 1.183 | - | - | - | 1.183 | 1.183 |

**[Table/Fig-4]:** Mean ADC values for liver lesions.

was used to determine sensitivity and specificity. With 1.431x$10^{-3}$ mm²/s cut off, the sensitivity of 87.5% (35/40), specificity of 71% (22/31), positive predictive value of 79.5% (35/44) and negative predictive value of 81.5% (22/27) were obtained.

Although abscesses are benign lesions, they showed restricted diffusion. Excluding abscesses, ADC cut-off value of 1.4819x$10^{-3}$ mm²/s was obtained by normal distribution (mean±2SD). ROC curve analysis (MedCalc v12.7.5.0 per Delong et al., [18] 1988 method) was used to determine sensitivity and specificity. With 1.4819x$10^{-3}$ mm²/s cut off, the sensitivity of 95% (38/40), specificity of 88% (22/25), positive predictive value of 92.7% (38/41) and negative predictive value of 91.7% (22/24) were obtained.

## DISCUSSION

For the current study total of 50 patients (71 liver lesions) were investigated. Clinical history, diagnostic modalities like biopsy/ FNAC, laboratory findings (AFP level etc.,) and other imaging modalities like USG, CT Scan; wherever applicable were taken into consideration for final diagnosis of liver lesions. For patients with multiple liver lesions, two or three lesions were considered. In the current study, all focal liver lesions showed higher signal intensity compared to surrounding liver parenchyma, predominantly on lower b value DWI images, enabling lesion detection. Further DWI in different b values along with generated ADC maps were used for further characterization of liver lesions.

In the present study, all malignant lesions including HCCs [Table/ Fig-5] and metastatic lesions [Table/Fig-6] showed restricted

Case Of Hepatocellular Carcinoma

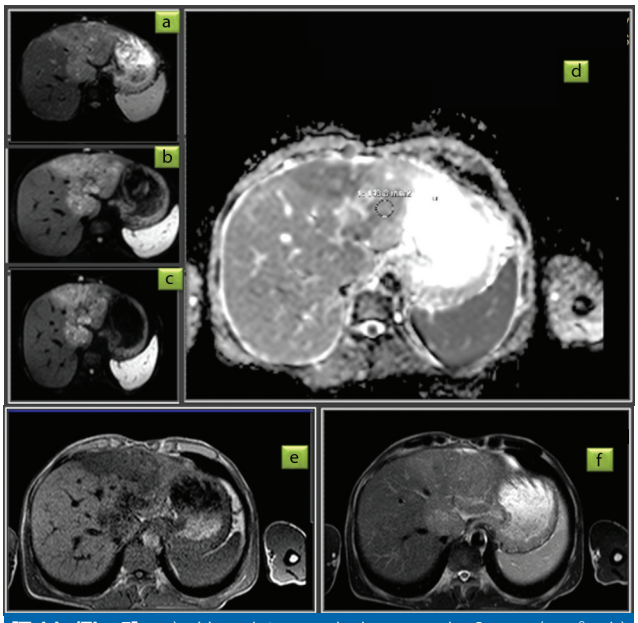


**[Table/Fig-5]:** a) Hyperintense lesion on b=0 sec/mm²; b) hyperintense lesion on b=500 sec/mm²; c) hyperintense lesion on b=1000 sec/mm²; d) hypointense lesion on ADC map, ADC=1.236 x $10^{-3}$ mm²/sec; e) Hypointense on T1WI; f) Hyperintense on T2WI. Final diagnosis was confirmed by FNAC, IHC & AFP level (12450 IU/ml).

Case of Hepatic Metastasis

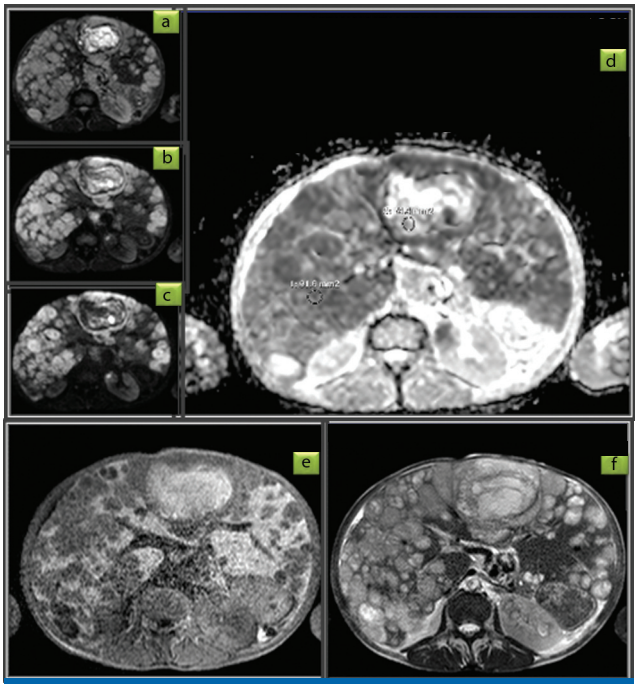


**[Table/Fig-6]:** a) Hyperintense lesions on b=0 sec/mm²; b) hyperintense lesions on b=500 sec/mm²; c) hyperintense lesions on b=1000 sec/mm²; d) hypointense lesions on ADC map, ADC=0.97 x $10^{-3}$ mm²/sec & ADC=1.45 x $10^{-3}$ mm²/sec; e&f) T1WI, T2WI images showing multiple liver metastasis. FNAC proven case of hepatic metastases of retroperitoneal liposarcoma.

diffusion. Heterogeneous hyperintense (DWI)/heterogeneous hypointense (ADC map) signal was seen predominantly in necrotic lesions. These results are comparable with study by Hosny et al., [19], which shows that there was persistent hyperintense signal of solid tumors on high b value DWI images. Badawy et al., [20] in his study concluded that all the malignant liver lesions show restricted diffusion suggested by persistent high signal at higher b values with corresponding low signal on ADC. Parikh et al., [21] too demonstrated that lesion is considered as malignant if it showed hyperintense signal at b=500sec/mm$^2$ & an ADC qualitatively lower than that of surrounding liver. Current study results concur with the same. Current study findings are similar to Scurr et al., [22], who found that colorectal liver metastases showed rim high signal intensity, uniform high signal intensity or variegate high signal intensity at b value of 500 sec/mm$^2$ on DW-MRI.

All hemangiomas [Table/Fig-7] showed no restricted diffusion on ADC. Persistence of hyperintense signal on higher 'b' values could be due to T2 shine through effect (validated by signal intensity on ADC map). According to Mazroa et al., [23], all hemangiomas show persistent hyperintense signal at increasing b values and also they show hyperintense or mixed signal on ADC maps suggesting T2 shine through. All simple cysts disappeared at b=1000sec/mm$^2$ and showed hyperintense signal intensity on ADC map. Inan et al., [24] found that at b=1000sec/mm$^2$, most simple cysts (93%) were isointense with liver and showed hyperintense signal on ADC map. Current study results are comparable with Inan et al., [24] and Hosny [19]. All abscesses (6 lesions, [Table/Fig-8] showed heterogeneous hyperintense signal intensity at b=500 sec/mm$^2$ and b=1000 sec/mm$^2$ and showed heterogeneous hypointense signal intensity on ADC map (restricted diffusion). Chan et al., [25] showed that all abscesses showed hyperintensity on DWI and hypointensity on ADC maps. All the hydatid cysts (2 lesions) disappeared at b=1000 sec/mm$^2$ and showed hyperintense signal intensity on ADC map (no restricted diffusion). Adenoma showed isointense signal intensity on DWI as well as ADC map (no restricted diffusion).

All 40 malignant lesions, 8 hemangiomas and all abscesses (2 lesions) showed persistent hyperintense/heterogeneous hyperintense signal intensity on DWI at higher 'b' values. Rest of the benign lesions disappeared at higher 'b' values (b=500 sec/mm$^2$ and/or b=1000 sec/mm$^2$).These results are similar to those obtained by Hosny [19]. Comparing DWI images and ADC map, all malignant lesions showed restricted diffusion. 19.4% of benign lesions (abscesses) showed restricted diffusion. Rest 77.4% benign lesions did not show restricted

**Case of Hepatic Hemangioma**

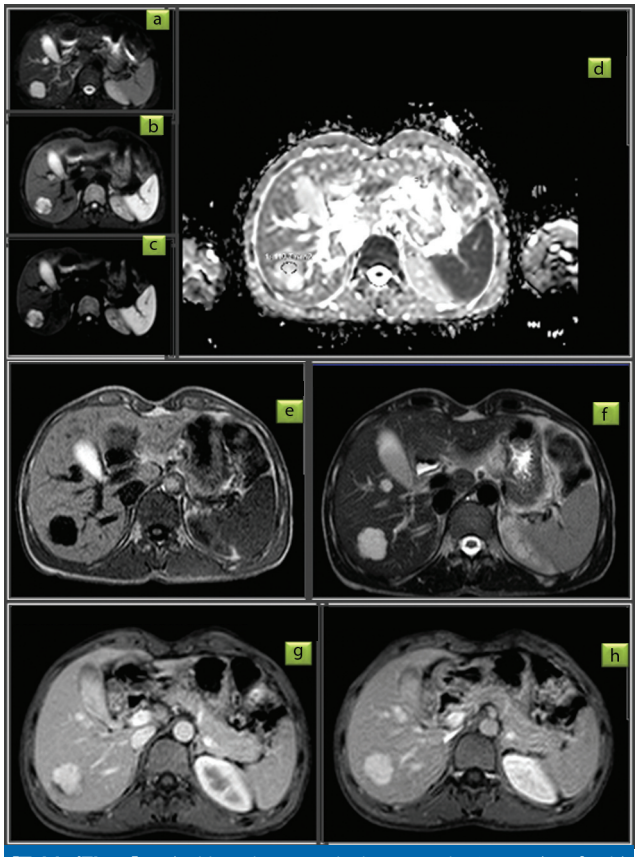


**[Table/Fig-7]:** a) Hyperintense lesion on b=0 sec/mm$^2$; b) hyperintense lesion on b=500 sec/mm$^2$; c) hyperintense lesion on b=1000 sec/mm$^2$; d) hyperintense lesion on ADC map, ADC=2.164 x 10$^{-3}$ mm$^2$/sec; e) Hypointense on T1WI; f) Hyperintense on T2WI; g&h) Post contrast images showing delayed centripetal enhancement.

**Case of Hepatic Abscess**

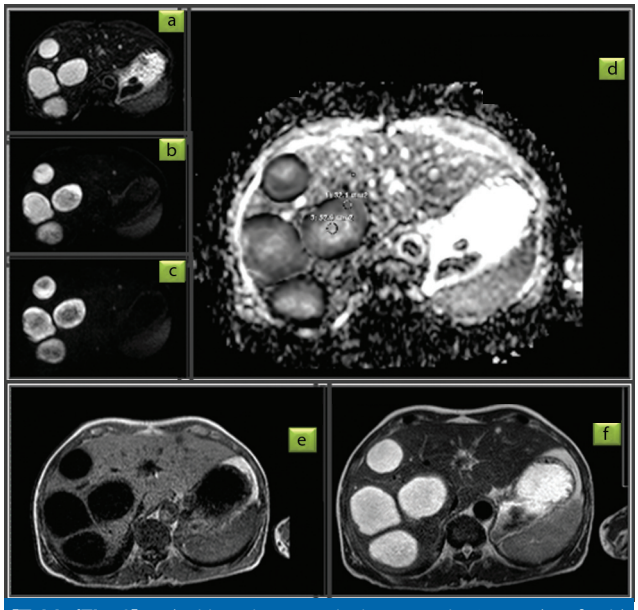


**[Table/Fig-8]:** a) Hyperintense lesion on b=0 sec/mm$^2$; b) Hyperintense lesion on b=500 sec/mm$^2$; c) Hyperintense lesion on b=1000 sec/mm$^2$; d) Hypointense lesion on ADC map, ADC=0.95 x 10$^{-3}$ mm$^2$/sec (average of ADCs in centre & periphery of lesion); e) Hypointense on T1WI; f) Hyperintense on T2WI.

| Parameter | Kim et al., [9] | Taouli et al., [15] | Demir et al., [1] | Bruegel et al., [7] | Parikh et al., [10] | Vergara et al., [13] | Current study |
|---|---|---|---|---|---|---|---|
| **No of patients/lesions** | 126/79 | 66/52 | 30/41 | 102/204 | 53/211 | 26/51 | 50/71 |
| **b values (sec/mm²)** | 0, 846 | 0, 500 | 0, 1000 | 50, 300, 600 | 0, 50, 500 | 50, 200, 400, 500, 700,850 | 0, 500, 1000 |
| | ADC Values (in $10^{-3}$ mm²/s) | | | | | | |
| **Metastases** | 1.06-1.11 | 0.94 | 0.79 ± 0.11 | 1.22 | 1.5 | 1.03 | 1.137 |
| **HCC** | 0.097-1.28 | 1.33 | 0.90 ± 0.10 | 1.05 | 1.3 | 1.08 | 0.975 |
| **Hemangioma** | 2.042-2.10 | 2.95 | 2.46 ± 0.21 | 1.92 | 2.04 | 1.68 | 1.689 |
| **Cyst** | 2.91-3.03 | 3.63 | 3.05 ± 0.26 | 3.02 | 2.54 | NA | 2.342 |
| **Adenoma/FNH** | NA | 1.75 | Na | 1.4 | 1.49 | 1.3 | 1.183 |
| **Benign lesions*** | 2.49 | 2.45 | 2.57 ± 0.26 | NA | 2.19 | 1.54 | 2.112 |
| **Malignant lesions** | 1.01 | 1.08 | 0.86 ± 0.11 | NA | 1.39 | 1.04 | 1.08 |
| **ADC cut-off*** | 1.6 | 1.5 | NA | 1.63 | 1.6 | 1.28 | 1.482 |
| **Sensitivity%*** | 98 | 84 | NA | 90 | 74 | 84 | 95 |
| **Specificity %*** | 80 | 89 | NA | 86 | 77 | 84 | 88 |

**[Table/Fig-9]:** Shows that current study is in concurrence with literature studied. Current study shows results similar to those reported by Hosny [18], Emara et al., [30] and Badawy et al., [19].
*Represents ADC values determined excluding abscesses.

diffusion. These results are comparable with Kilickesmez et al., [26] who demonstrated that lesions with high cellularity like tumors show restricted diffusion while those with low cellularity like cysts do not show restricted diffusion. Similar results were also obtained in study done by Hosny [19].

For the statistical calculations MedCalc v12.7.5.0 was used in current study. Among total 71 lesions, it was observed that benign lesions had highest mean ADC value. Hydatid cyst had max mean ADC value of $2.981\times10^{-3}$ mm²/sec followed by simple cysts having $2.342\times10^{-3}$ mm²/sec. Among malignant lesions, HCC had the lowest mean ADC value of $0.975\times10^{-3}$ mm²/sec while metastases had mean ADC value of $1.137\times10^{-3}$ mm²/sec. Although being benign lesions, abscesses had mean ADC value of $0.879\times10^{-3}$ mm²/sec. Mean ADC value for benign lesions was $1.87\times10^{-3}$ mm²/sec and for malignant $1.08\times10^{-3}$ mm²/sec. Using Independent sample t-test; p-value < 0.05 therefore there was significant difference between mean ADC values for malignant lesions and benign lesions in the studied samples. Similarly using Independent sample Welch-test for unequal variances; p-value < 0.05 therefore there was significant difference between mean ADC values for HCC and metastases. Taouli et al., [27] showed that in one of imaging sequence, HCCs and metastases had significant differences between mean ADC values.

Above observations are similar with findings of Hosny [18], who showed that cysts and hemangiomas had highest ADC values while malignant masses had the lowest. Similarly Ischikawa et al., [28] stated that hemangiomas showed higher ADCs than HCC and metastases. In the study done by Sun et al., [29], mean ADC value of HCC was $0.95\pm0.11\times10^{-3}$ mm²/sec and that of metastases was $1.13\pm0.21\times10^{-3}$ mm²/sec. Similar results were obtained in current study. ADC cut-off value of $1.431\times10^{-3}$ mm²/s was obtained by normal distribution (mean±2SD). Sensitivity of 87.5% (35/40), specificity of 71% (22/31), positive predictive value of 79.5% (35/44) and negative predictive value of 81.5% (22/27) were obtained. Excluding abscesses, ADC cut-off value of $1.4819\times10^{-3}$ mm²/s was obtained by normal distribution (mean±2SD). Sensitivity of 95% (38/40), specificity of 88% (22/25), positive predictive value of 92.7% (38/41) and negative predictive value of 91.7% (22/24) were obtained.

Demir et al., [30] showed that mean ADC value for abscess was $1.09\pm0.32\times10^{-3}$ mm²/sec. He explained that this low value could be related to dense viscous content of abscess. According study by Chan et al., [25] mean ADC value was significantly lower for hepatic abscess compared to necrotic tumors and simple cyst ($0.67\pm0.35\times10^{-3}$ mm²/sec). Current study shows comparable results with literature studies. Study by Demir et al., [30] shows that hydatid cysts have a mean ADC value of $2.99\pm0.24\times10^{-3}$ mm²/sec, which was similar to simple cyst. According to Kilickesmez et al., [26] mean ADC value of hydatid cysts was $2.58\pm0.53\times10^{-3}$ mm²/sec. This value was not significantly different from simple cyst. Current study results concur with above literature studies [Table/Fig-9].

## LIMITATIONS

Sample size and duration of study was small. Being oncology setup, number of malignant lesions was more than benign lesions and pediatric population was excluded from study.

Not all cases had pathological confirmation; hence alternative confirmative methods like USG/CT/AFP levels were used. Contrast study was not done in most of the cases due to poor socio-economic status of most of the patients.

Qualitative and quantitative assessment of liver lesions was done based on only diffusion-weighted MR imaging. Comparison with conventional MR imaging was not done.

### Pitfalls of DWI

Higher b values cause lower quality on DWI and make evaluation harder.

Single Shot SE echoplanar DW MRI has limited image quality, including poor SNR, limited spatial resolution and echoplanar imaging related artifacts.

## CONCLUSION

Based on qualitative and quantitative assessment of liver lesions on DWI and ADC map, we could characterize different liver lesions. In same way differentiation between malignant & benign lesions as well as HCC & metastases was done. DWI is a useful diagnostic tool in patients where contrast is contraindicated like in patients with renal impairment. Need of FNAC/biopsy for differentiating between benign and malignant lesion can be mitigated using DWI. Small or deeply situated lesions where FNAC is not accessible, DWI technique acts as powerful diagnostic tool. However DWI should always be interpreted with conventional MRI sequences due to overlap between ADC values of different liver lesions.

## REFERENCES


[1] Marrero JA, Ahn J, Rajender Reddy K. ACG clinical guideline: the diagnosis and management of focal liver lesions. *Am J Gastroenterol.* 2014;109:1328-47.

[2] Dietrich CF, Kratzer W, Strobe D, et al. Assessment of metastatic liver disease in patients with primary extrahepatic tumors by contrast enhanced sonography versus CT and MRI. *World J Gastroenterol.* 2006;12:1699-05.

[3] Dietrich CF, Sharma M, Gibson RN, Schreiber-Dietrich D, Jenssen C. Fortuitously discovered liver lesions. *World J Gastroenterol.* 2013;19:3173-88.

[4] Galea N, Cantisani V, Taouli B. Liver lesion detection and characterization: role of diffusion-weighted imaging. *J Magn Reson Imaging*. 2013;37:1260-76.

[5] Chiorean L, Cantisani V, Jenssen C, Sidhu PS, Baum U, Dietrich CF. Focal masses in a non-cirrhotic liver: The additional benefit of CEUS over baseline imaging. *Eur J Radiol*. 2015;84(9):1636-43.

[6] Furukawa MKK, Kamada H, Miyasaka K. MRI in seven cases of tacrolimus (FK-506) encephalopathy: utility of FLAIR and diffusion-weighted imaging. *Neuroradiology*. 2001;43:615–21.

[7] Berman JI. Diffusion tensor imaging-guided tracking of fibers of the pyramidal tract combined with intraoperative cortical stimulation mapping in patients with gliomas. *J Neurosurg*. 2004;101:66–72.

[8] Takeuchi MNH, Mori K, Sakama M. Magnetic resonance imaging and proton MR spectroscopy of the brain in a patient with carbohydrate deficient glycoprotein syndrome type I. *J Magn Reson Imaging*. 2003;17:722–25.

[9] DTB M. Diffuse liver disease: Strategies for hepatic CT and MR imaging. *Radiographics*. 2009;29:1591–614.

[10] Koh DM, Collins DJ. Diffusion-weighted MRI in the body:applications and challenges in oncology. *AJR*. 2007;188:1622–35.

[11] Stejskal EO, Tanner JE. Spin diffusion measurements: spin echoes in the presence of a time-dependent field gradient. *J Chem Phys.* 1965;42:288–92.

[12] Luypaert R, Boujraf S, Sourbron S, Osteaux M. Diffusion and perfusion MRI: basic physics. *Eur J Radiol.* 2001;38:19-27.

[13] Le Bihan D, Breton E, Lallemand D, Grenier P, Cabanis P, Laval –Jeantet M. MR imaging of intravoxel incoherent motions: application to diffusion and perfusion in neurologic disorders. *Radiology.* 1986;161:401–07.

[14] Bammer R. Basic principles of diffusion-weighted imaging. *Eur J Radiol.* 2003;45:169-84.

[15] Le Bihan D, Breton E, Lallemand D, Aubin ML, Vignaud J, Laval-Jeantet M. Separation of diffusion and perfusion in intravoxel incoherent motion MR imaging. *Radiology*. 1988;168:497-505.

[16] Taouli B, Koh DM. Diffusion-weighted MR imaging of the liver. *Radiology.* 2010; 254(1):47-66.

[17] Qayyum A. Diffusion-weighted imaging in the abdomen and pelvis: Concepts and applications. *Radio Graphics.* 2009;29:1797-810.

[18] DeLong ER, DeLong DM, Clarke-Pearson DL. Comparing areas under two or more correlated reciever operating characteristics curves: a nonparamentric approach. *Biometrics*. 1988;44(3):837–45.

[19] Hosny IA. Diffusion MRI of focal liver lesions. *PJR.* 2010; 20:01-07.

[20] Badawy ME, Hamesa M, Elaggan A, Nooman AE, Gabr M. Can diffusion-weighted MRI differentiate between benign and malignant hepatic focal liver lesion? *Egypt J Radiol Nucl Med*. 2013;44:453-61.

[21] Parikh T, Drew SJ, Lee VS, Wong S, Hecht EM et al. Focal liver lesion detection and characterization with diffusion-weighted MR imaging: comparison with standard breath-hold T2-weighted imaging. *Radiology.* 2008;246 (3) : 812–22.

[22] Scurr ED, Collins DJ, Temple L, Karanjia N, Leach MO, Koh D-M. Appearance of colorectal hepatic metastases at diffusion-weighted MRI compared with histopathology: Initial observations. *Br J Radiol*. 2012;85: 225-30.

[23] Mazroa JA, Elmogy SA. Typical and atypical liver hemangiomas. Can diffusion MR with different b values provide confident diagnosis? *Egypt J RadiolNucl Med*. 2011;42:357-65.

[24] Inan N, Arslan A, Akansel G, Anik Y, Sarisoy HT, Ciftci E et al. Diffusion-weighted imaging in differential diagnosis of simple and hydatid cysts of liver. *AJR Am J Roentgenol*. 2007;189:1031-36.

[25] Chan JHM, Tsui EYK, Luk SH, Fung ASL, Yuen MK et al. Diffusion-weighted MR imaging of the liver: distinguishing hepatic abscess from cystic or necrotic tumor. *Abdom Imaging*. 2001;26:161–65.

[26] Kilickesmez O, Bayramoglu S, Inci E, Cimilli T. Value of apparent diffusion coefficient measurement for discrimination of focal benign and malignant hepatic masses. *J Med Imaging Radiat Oncol.* 2009;53:50-55.

[27] Taouli B, Vilgrain V, Dumont E, Daire J, Fan B, Menu Y. Evaluation of liver diffusion isotropy and characterization of focal hepatic lesions with two single-shot echo-planar MR imaging sequences: prospective study in 66 patients. *Radiology*. 2003;226:71–78.

[28] Ichikawa T, Haradome H, Hachiya J, Nitatori T, Araki T. Diffusion-weighted MR imaging with a single-shot echoplanar sequence:

detection and characterization of focal hepatic lesions. *AJR Am J Roentgenol.* 1998;170:397-402.

[29] Sun XJ, Quan XY, Huang FH, Xu YK. Quantitative evaluation of diffusion-weighted magnetic resonance imaging of focal hepatic lesions. *World J Gastroenterol.* 2005;11(41):6535–37.

[30] Demir Öl, Obuz F, Sagol Ö, Dicle O. Contribution of diffusion-weighted MRI to the differential diagnosis of hepatic masses. *Diagn Interv Radiol*. 2007; 13:81-86.

**AUTHOR(S):**

1. Dr. Madhu SD
2. Dr. Jaipal R Beerappa
3. Dr. Pooja
4. Dr. Raghuram P

**PARTICULARS OF CONTRIBUTORS:**

1. Assistant Professor, Department of Radio-Diagnosis. Kidwai Memorial Institute of Oncology, Bengaluru, India.
2. Associate Professor, Department of Radio-Diagnosis. Kidwai Memorial Institute of Oncology, Bengaluru, India.
3. Post graduate, Department of Radio-Diagnosis. Kidwai Memorial Institute of Oncology, Bengaluru, India.
4. Professor, Department of Radio-Diagnosis. Kidwai Memorial Institute of Oncology, Bengaluru, India.

**NAME, ADDRESS, E-MAIL ID OF THE CORRESPONDING AUTHOR:**

Dr. Madhu SD,
No 20/A, 6th A Main, 11th cross, 3rd Phase JP Nagar,
Bangalore-560078, India.
E-mail: sdmadhudoc@gmail.com

**FINANCIAL OR OTHER COMPETING INTERESTS:** None.

Date of Publishing: **Jul 01, 2016**